

# Strong adhesion in nanocrystalline diamond films on silicon substrates

T. Sharda and M. Umeno

*Research Center for Micro-Structure Devices, Nagoya Institute of Technology, Gokiso-cho, Showa-ku, Nagoya 466 8555, Japan*

T. Soga<sup>a)</sup> and T. Jimbo

*Department of Environmental Technology and Urban Planning, Nagoya Institute of Technology, Gokiso-cho, Showa-ku, Nagoya 466 8555, Japan*

(Received 7 September 2000; accepted for publication 30 January 2001)

Strong adhesion is shown to be achieved in the growth of smooth nanocrystalline diamond (NCD) thin films on silicon substrates at 600 °C using biased enhanced growth in microwave plasma chemical vapor deposition. The strong adhesion is evident from the films sustaining compressive stress, which may be as high as 85 GPa. The substrates are bent spherically after deposition, however, films are not peeled off, in spite of having enormous in-plane stress. The strong adhesion may be a result of implanted carbon below the substrate surface with an optimized ion flux density in the initial stages of growth. The compressive stress in the films is shown to be generating from the graphitic and other nondiamond carbon impurities in the films. It was observed that the NCD grain size decreases with biasing hence increasing grain boundary area in the films accommodating more graphitic impurities, which in turn results in an increase in compressive stress in the films.

© 2001 American Institute of Physics. [DOI: 10.1063/1.1358318]

## I. INTRODUCTION

Wear on machinery can be considered as one of the biggest problems faced by industries, which causes the largest expenses too. Diamond is considered the best wear-resistant material. An excellent combination of diamond properties, for instance its high hardness and low friction coefficient with its high thermal conductivity, makes diamond the best candidate for wear-resistant applications. However, conventional chemical vapor deposited (CVD) diamond coatings that are deposited at high temperatures have rough surfaces. The high surface roughness is a major problem when using diamond films for machining and wear applications.<sup>1,2</sup> In fact, high surface roughness limits uses of diamond films in other fields also. For example, diamond is well suited for use as protective optical coatings but diamond films with high surface roughness cause attenuation and scattering of the transmitted signals restricting their uses in optical coatings. In order to overcome the problem of surface roughness of diamond films either post-polishing should be adopted or naturally smooth films should be grown without compromising their hardness and other useful properties much. However, post-polishing is expensive and time consuming<sup>3-5</sup> and it will be better to concentrate on growing naturally smooth films.<sup>4,6-9</sup>

Nanocrystalline or amorphous diamond, tetrahedral amorphous carbon (ta-C), and diamond like carbon (DLC) films are much smoother, equally hard as conventional diamond, and can be grown at lower temperatures.<sup>10-13</sup> However, the nanocrystalline diamond (NCD) and related films contain a high level of compressive stress (2–15 GPa) within the planes of the films.<sup>14-20</sup> The stress in the films directly

affects their adhesion and causes them to delaminate from the substrate.<sup>18</sup> This in turn restricts the film thickness to a few tens of nanometers to keep the film stable on the substrate. This thickness is too low to use the films for tribological applications and also higher stress cannot be developed beyond 10–12 GPa for fundamental studies. The current research in this area in various laboratories and universities is aimed to reduce this stress and, at the same time, to improve adhesion of these films to the substrate.

Most of the reports on ta-C and DLC observed stress not more than 10–12 GPa.<sup>15,19</sup> This is mainly because the adhesion of the film to the substrate cannot sustain this amount of stress, resulting in delamination of the film. Efforts have been concentrated, so far, in reducing the high amount of the stress from the film rather than improving upon the adhesion to sustain even higher stress of the films.<sup>12,13,18</sup> It is reported by several groups that the films peel off from the substrates after some time of deposition if the stress in the film exceeds even 2 GPa.<sup>17,18</sup> After the films peel off at this amount of stress, further growth cannot be continued and, in turn, higher stress cannot be observed. In the present article we show the highest ever reported amount of compressive stress in our smooth nanocrystalline diamond (NCD) films. The high amount of stress could be observed in our films as a result of strong adhesion of the films to the substrates sustaining enormous stress.

We believe that if the carbon can be implanted deep inside the substrate with an optimized ion density and if the growth is continued leading to a film, it may be possible to develop strong adhesion of the films to the substrates. Implantation of carbon inside the substrate surface may be possible with a subplantation mechanism, described originally by Liflitz *et al.*<sup>21</sup> and later supported by various groups in the area of diamond and related materials.<sup>18,22</sup> In our study also,

<sup>a)</sup>Electronic mail: soga@elcom.nitech.ac.jp

we showed that NCD could be grown by biased enhanced growth (BEG),<sup>6,7</sup> which was shown to be a result of the subplantation mechanism with additional effects of temperature and atomic hydrogen concentration. In the present study we show that the concept of implanting carbon below the silicon substrate in the initial stages of the growth works well in order to improve the adhesion. As a result, we could observe stress, which may be as high as 85 GPa and, to our surprise, the films are still adhered to the substrates, even after several months of deposition.

## II. EXPERIMENT

The nanocrystalline diamond films were grown in a 2.45 GHz Applied Science and Technology (ASTeX) made microwave plasma CVD (MPCVD) system. The mirror polished Si(100) substrates were kept on a molybdenum holder. No diamond powder or any other *ex situ* treatment was performed prior to the depositions. The substrate assembly was immersed in methane and hydrogen plasma. Three sets of films were grown while applying negative dc bias voltages of 200, 260, and 320 V to the substrates with respect to the chamber that was grounded. A special arrangement was made to let the whole ion current pass through the substrate. A mixture of 5% CH<sub>4</sub> in H<sub>2</sub> was used at a pressure of 30 Torr, with a microwave power of 1000 W. The substrate was held at a constant temperature of 600 °C throughout the deposition. The whole growth was performed for 1 h in a single stage run without breaking the bias to the substrate, unlike the conventional two or three stage process for the heteroepitaxial growth of diamond.<sup>22,23</sup> This is the reason to term the growth, in the present study, as BEG. The thickness of the films varies in the range from 1000 to 1900 nm. The rms value of the minimum surface roughness in the films, evaluated by atomic force microscopy, was ~17 nm. Substrates, after the depositions, were bent spherically due to high stress in the plane of the films. As the after deposited samples were bent concave in the shape with the films side up, the stress is compressive in nature.

Stress in the films was estimated by measuring the curvature of the films on substrates using an Alpha-500 profilometer. The thickness was calculated by a UV reflection pattern of the films assuming the refractive index as 2. Hardness of the films was measured by a nano-indenter (UMIS-2000). Structural characterizations of the films were carried out using Raman spectroscopy, x-ray diffraction (XRD), and atomic force microscopy. The laser Raman spectra were obtained in the range 1000–1700 cm<sup>-1</sup> with a step size of 1 cm<sup>-1</sup>. An Ar<sup>+</sup> laser ( $\lambda=488$  nm) of 200  $\mu\text{m}$  diameter spot size was used for recording the spectra. The estimated laser power at the sample was 20 mW. The XRD measurements were performed from a computer controlled XRD machine using Cu K $\alpha$  radiation to find the crystalline structures of the films.

## III. RESULTS AND DISCUSSION

The stress in the films was calculated by measuring the radius of curvature of the substrates before and after the deposition using the modified Stoney's equation.<sup>24</sup> The sub-

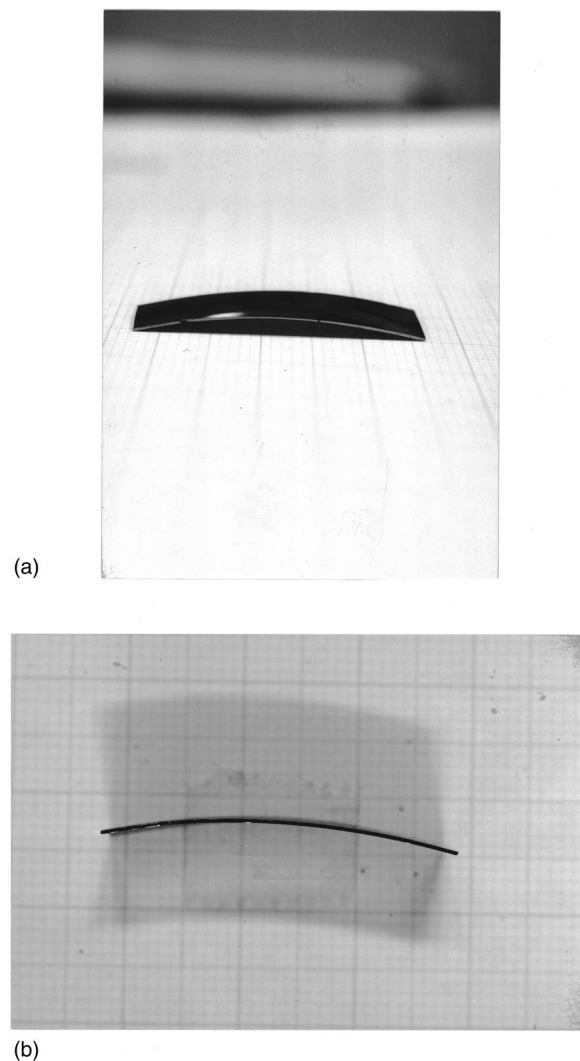


FIG. 1. (a) and (b) Photographs of a bent sample as viewed from different angles.

strates after the deposition at 320 V were visibly bent, as seen from different viewing angles in Figs. 1(a) and 1(b), which accounts for an enormous stress in the films, which was estimated to be about 85 GPa. To the best of our knowledge, there is no report on such a high amount of stress in carbon films. It may be mainly because the films deposited by other groups delaminated soon after the deposition in the case of more than 2 GPa compressive stress due to weak adhesion.<sup>17,18</sup> However, in our case, it may be due to strong adhesion of the films to the substrate that we could observe such an enormous stress. The stress in the films is plotted as a function of bias voltage in Fig. 2. The amount of the stress increases with bias and shoots up in the film grown at 320 V. The hardness of the films, measured by a nano-indenter, is also plotted in Fig. 2 as a function of bias. The hardness of the films decreases with an increase in bias unlike the case of ta-C. In the later, hardness and stress follow the same trend with conditions.<sup>18–20</sup>

Figure 3 shows the Raman spectra of the films deposited on Si(100). The Raman features of the samples mainly exhibit three clearly distinct broad bands, at least in the case of

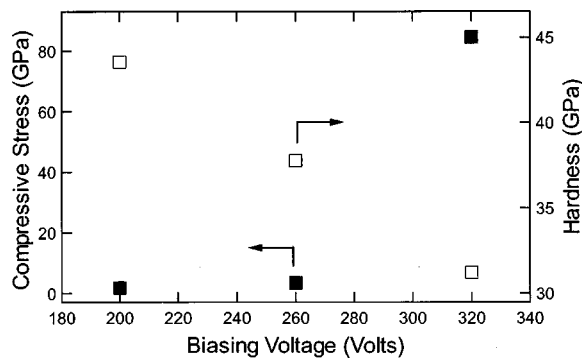


FIG. 2. Plot of compressive stress and hardness as a function of biasing voltage. An error in the calculation of stress measurement will arise from the deviation in the refractive index of the films, which is assumed to be 2 but may vary in the range from 1.8 to 2.4. Hardness data presented in the graph is averaged from a few sets of five indents on the samples.

the films grown at 200 and 260 V. The positions of the broad bands in the spectra of the films, as shown in the figure, are near 1150, 1350, and 1550  $\text{cm}^{-1}$ . The band near 1150  $\text{cm}^{-1}$  is shown to be related to the calculated phonon density of states of diamond and has been assigned to the presence of the nanocrystalline phase of diamond.<sup>25,26</sup> Various other groups have observed it repeatedly in the amorphous and NCD films.<sup>9,27–29</sup> It has also been observed as a weak band in the microcrystalline diamond films along with a sharp peak near 1332  $\text{cm}^{-1}$ , an unambiguous signature of crystalline cubic diamond.<sup>9,27,30</sup> It is interesting to note that though the films grown at 200 and 260 V show an intense band related to NCD, they do not show any peak near 1332  $\text{cm}^{-1}$ . This could be a sign of uniformly distributed short-range  $sp^3$  crystallites in the films.<sup>25,27,29</sup> The Raman features of our films match with the Raman features of amorphous diamond grown using low energy cluster beam deposition of carbon clusters with size distribution centered around  $C_{20}$  (Ref. 25)

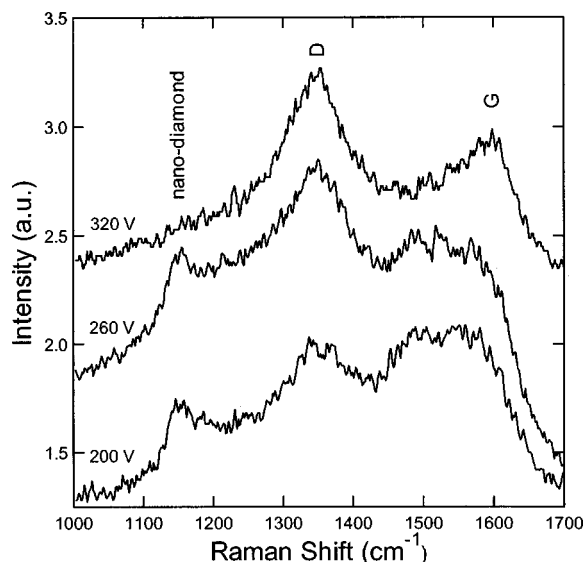


FIG. 3. Raman spectra of the films deposited at different biasing voltages. The samples were excited by a 488 nm  $\text{Ar}^+$  laser. The three distinct bands near 1150, 1350, and 1580  $\text{cm}^{-1}$  correspond to nano-diamond (NCD), graphitic  $D$  and  $G$  bands, respectively.

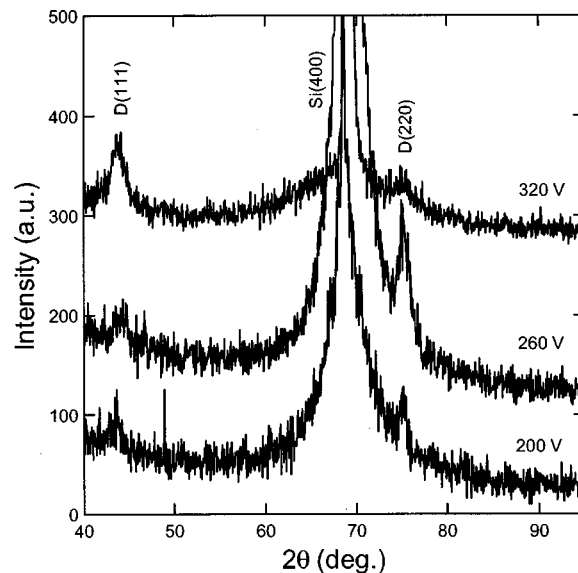


FIG. 4. XRD patterns of the films deposited at different biasing voltages. The reflections from (111) and (220) planes of cubic diamond are evident in the films grown on Si substrates. Grain size of the NCD grains was estimated from the FWHM and position of the diamond (111) and (220) peaks (see Ref. 34).

and also with NCD grown by MPCVD on Si substrates abraded by diamond powder.<sup>9,27</sup> It was shown in the former study that the clusters keep the memory effect and, as  $C_{20}$  clusters are  $sp^3$  hybridized, the deposit turns out to be diamond in amorphous form. The later studies showed the use of a high concentration of Ar in  $\text{Ar}/\text{H}_2/\text{CH}_4$  microwave plasmas<sup>9</sup> and the use of  $\text{CO}/\text{H}_2$  mixtures for the growth of NCD on the seeded Si surface.<sup>27</sup> At the same time, Raman features of our films do not match with the Raman features of NCD synthesized from transformation of  $C_{60}$ .<sup>31</sup> Hirari *et al.*<sup>31</sup> observed only a cubic diamond feature in their film. Other bands in the Raman spectra of our films near 1350 and 1580  $\text{cm}^{-1}$  (Fig. 3) are popularly known as  $D$  and  $G$  bands, which are related with graphitic islands.<sup>30</sup> The  $D$  band appears due to the relaxation in the momentum selection rules of the Raman scattering process due to the small domain size in graphite. In fact, a similar argument is applicable to the appearance of the band near 1140  $\text{cm}^{-1}$  due to nanocrystallinity of diamond.<sup>30</sup> However, the higher or equal intensities of the graphitic bands in Fig. 3 in the films grown at 200 and 260 V, as compared to the intensity of the nanocrystalline diamond band, do not represent a high amount of  $sp^2$  carbon in those films. This is because the cross section of Raman scattering is 50–60 times higher for  $sp^2$ -bonded carbon as compared to  $sp^3$ -bonded carbon, as reported by Wada *et al.*<sup>32</sup> This small amount of graphitic carbon in our films may exist between the nano-diamond grains,<sup>33</sup> i.e., on the grain boundaries. As can be seen, the intensity of the nanocrystalline peak decreases in the spectra with an increase in bias voltage, in fact it has almost vanished in the films grown at 320 V. Also, there is a drastic variation in the position of the graphitic  $G$  band in the films grown at 320 V. It indicates that the relative concentration of  $sp^3$  to  $sp^2$  carbon of the films decreases with biasing voltage in the films.

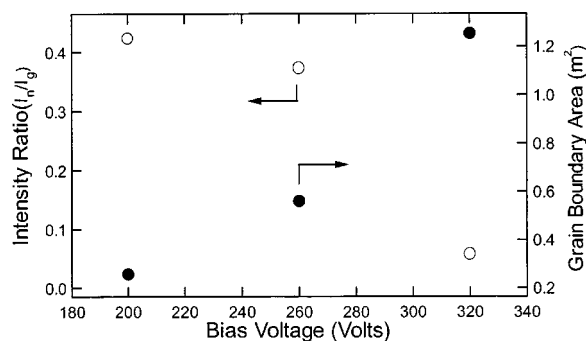


FIG. 5. Plot of the Raman intensity ratio NCD ( $I_n$ ) to graphitic  $G$  band ( $I_g$ ) and grain boundary area of NCD grains as a function of biasing voltage. Clearly, the concentration of NCD decreases and the grain boundary area increases as NCD grain increases with biasing voltage.

XRD was performed in the  $2\theta$  range from  $40^\circ$  to  $95^\circ$ . Figure 4 shows the XRD patterns of the films. The calculated interplanar spacing corresponding to the peaks at  $2\theta \sim 44.05^\circ$  and  $75.25^\circ \pm 0.20^\circ$  in the XRD patterns of the films match closely with the interplanar  $d$ -values of (111) and (220) planes of cubic diamond, respectively. It should be noted that the full width at half maximum (FWHM) of the diamond peaks in the films is in general high as compared to the CVD grown microcrystalline films. This is well correlated with the fact that diamond nanocrystallites<sup>9</sup> are present in our films. Although not shown, it should be noted that no peaks associated with graphite could be identified in our films. The films grown at 200 and 260 V show mostly the peak associated with the (220) plane of cubic diamond whereas the films grown at 320 V shows a broad peak associated with the (111) plane of cubic diamond.

The strong adhesion of the films to the substrates is evident from the films, grown at 320 V, sustaining enormous stress. As the films are not peeled off at such an enormous stress, it can be considered to be a result of strong adhesion of the films to the substrate. The strong adhesion in our films is a result of subplantation of carbon ions into the substrate in the initial stages of growth. The carbon ions are deposited into the substrate with energies suitable for efficient subplantation beneath the substrate surface when the deposition commences. It is estimated from the incubation period and growth rates that the implantation of the carbon ions could be more than 100–200 nm below the substrate surface. Implantation up to the thickness of 100–200 nm with an optimized flux density may be the key to strong adhesion in our films.

As shown in our previous work, growth of NCD at the conditions used in the present study can be explained in terms of the subplantation model with additional effects due to CVD diamond conditions.<sup>6,7</sup> Raman spectra and XRD patterns are sufficient evidence of the presence of NCD. However, Raman spectra also show considerable presence of graphitic carbon in the films, which increases with biasing voltage. The Raman intensity ratio of NCD ( $I_n$ ) to graphitic  $G$  band ( $I_g$ ) in the films is plotted as a function of biasing voltage in Fig. 5. The intensity of the NCD and graphitic band  $G$  was taken after peak fitting the Raman spectra using a standard computer peak-fit program. Clearly, the ratio

( $I_n/I_g$ ) decreases with biasing voltage indicating that the concentration of NCD with respect to the graphitic impurities in the films decreases with biasing voltage. It is quite probable that most of the graphitic and other nondiamond carbon impurities in the films are sticking at the grain boundaries.<sup>33</sup> As the specific volume of graphite is 1.5 times more than diamond, it may be that the graphitic carbon sticking at the NCD grain boundaries is responsible for the compressive stress in the films.<sup>33</sup> This means that the stress should vary with the grain boundary area (GBA) of the NCD grains. A crude estimation of diamond grain size was carried out using the FWHM of the XRD<sup>34</sup> diamond peaks. GBA in the total region of deposition ( $3 \times 3 \text{ cm}^2$ ) was estimated using the grain size of NCDs and assuming that the grains are cylindrical in shape. The estimated GBA is also plotted in Fig. 5 as a function of biasing voltage. As can be seen, the GBA increases substantially with biasing voltage. This matches well with the variation of the Raman intensity ratio  $I_n/I_g$  with biasing voltage, i.e., the higher the GBA, the higher is the concentration of graphitic impurities in the films. This supports the conjecture that the compressive stress in our films may be the result of graphitic impurities sticking at the NCD grain boundaries. Apart from nondiamond carbon impurities, it may be the amount of incorporated hydrogen generating compressive stress in the films. Although the two impurities (the H content and nondiamond carbon) in the films may be related to each other,<sup>35,36</sup> more measurements are needed to find out their specific roles in the generation of compressive stress in the films.

Alternatively it may be highly plausible that while the subplantation mechanism is applicable to our system, compressive stress could be the result of the energetic particles striking the growing film.<sup>14,37,38</sup> However, the steep increase in the stress while changing the voltage from 260 to 320 V could not be understood from the existing models. Also, in our films, hardness and compressive stress do not follow the same trend with deposition parameters as commonly observed in ta-C and DLC films.<sup>14,18–20</sup> Therefore it may be mainly the nondiamond carbon impurities sticking at the grain boundaries of the NCD grains responsible for the generation of compressive stress in the films.

#### IV. CONCLUSIONS

In conclusion, it is shown that a strong adhesion can be developed between the nanocrystalline diamond films and substrates that can sustain an enormous amount of stress in the films. It was observed that stress which may be as high as 85 GPa can exist in nanocrystalline diamond films. The graphitic carbon impurities sticking at the grain boundaries of nanocrystalline diamond is shown to be the main cause for high compressive stresses in the films.

#### ACKNOWLEDGMENTS

This work was supported by the Japan Society for Promotion of Science under the program ‘‘Research for the Future.’’ The authors gratefully acknowledge Professor M. Ichimura for Raman spectroscopy measurements for the present work.

- <sup>1</sup>D. G. Bhat *et al.*, *Diamond Relat. Mater.* **4**, 921 (1995).
- <sup>2</sup>A. K. Gangopadhyay and M. A. Tamor, *Wear* **169**, 221 (1993).
- <sup>3</sup>B. Bhusan, *Diamond Relat. Mater.* **8**, 1985 (1999).
- <sup>4</sup>A. Erdemir *et al.*, *Surf. Coat. Technol.* **120-121**, 565 (1999).
- <sup>5</sup>S. K. Choi, D. Y. Jung, S. Y. Kweon, and S. K. Jung, *Thin Solid Films* **279**, 110 (1996).
- <sup>6</sup>T. Sharda, T. Soga, T. Jimbo, and M. Umeno, *Diamond Relat. Mater.* **9**, 1331 (2000).
- <sup>7</sup>T. Sharda, T. Soga, T. Jimbo, and M. Umeno, *Appl. Phys. Lett.* **77**, 4304 (2000).
- <sup>8</sup>S. Hogmark, O. Hollman, A. Alahelisten, and O. Hedenqvist, *Wear* **200**, 225 (1996).
- <sup>9</sup>D. Zhou, T. G. McCauley, L. C. Qin, A. R. Krauss, and D. M. Gruen, *J. Appl. Phys.* **83**, 540 (1998).
- <sup>10</sup>F. Davanloo, H. Park, and C. B. Collins, *J. Mater. Res.* **11**, 2042 (1996).
- <sup>11</sup>C. B. Collins, F. Davanloo, T. J. Lee, H. Park, and J. H. You, *J. Vac. Sci. Technol. B* **11**, 1936 (1993).
- <sup>12</sup>T. A. Friedmann *et al.*, *Appl. Phys. Lett.* **71**, 3820 (1997).
- <sup>13</sup>M. Chhowalla, Y. Yin, G. A. J. Amaratunga, D. R. McKenzie, and Th. Fraurnheim, *Appl. Phys. Lett.* **69**, 2344 (1996).
- <sup>14</sup>D. R. Mckenzie, D. A. Muller, and B. A. Paithorpe, *Phys. Rev. Lett.* **67**, 773 (1991).
- <sup>15</sup>P. J. Fallon *et al.*, *Phys. Rev. B* **48**, 4777 (1993).
- <sup>16</sup>M. Weiler *et al.*, *Appl. Phys. Lett.* **64**, 2797 (1994).
- <sup>17</sup>F. C. Marques, R. G. Lacerda, G. Y. Odo, and C. M. Lepienski, *Thin Solid Films* **332**, 113 (1998).
- <sup>18</sup>R. G. Lacerda and F. C. Marques, *Appl. Phys. Lett.* **73**, 617 (1998).
- <sup>19</sup>S. Sattel, J. Robertson, M. Scheib, and H. Ehrhardt, *Appl. Phys. Lett.* **69**, 497 (1996).
- <sup>20</sup>S. Logothetidis, M. Gioti, P. Patsalas, and C. Charitidis, *Carbon* **37**, 765 (1999).
- <sup>21</sup>Y. Lifshitz, G. D. Lempert, and E. Grossman, *Phys. Rev. Lett.* **72**, 2753 (1994).
- <sup>22</sup>J. Robertson *et al.*, *Appl. Phys. Lett.* **66**, 3287 (1995).
- <sup>23</sup>X. Jiang, C.-P. Klages, R. Zachai, M. Hartweg, and H.-J. Fusser, *Appl. Phys. Lett.* **62**, 3438 (1993).
- <sup>24</sup>R. J. Jaccodine and W. A. Schlegel, *J. Appl. Phys.* **37**, 2429 (1966).
- <sup>25</sup>V. Paillard, P. Melinon, V. Dupuis, J. P. Perez, and A. Perez, *Phys. Rev. Lett.* **71**, 4170 (1993).
- <sup>26</sup>V. Paillard *et al.*, *Phys. Rev. B* **49**, 11433 (1994).
- <sup>27</sup>J. Lee, R. W. Collins, R. Messier, and Y. E. Strausser, *Appl. Phys. Lett.* **70**, 1527 (1997).
- <sup>28</sup>S. Logothetidis, *Appl. Phys. Lett.* **69**, 158 (1996).
- <sup>29</sup>S. A. Catledge and Y. K. Vohra, *J. Appl. Phys.* **84**, 6469 (1998).
- <sup>30</sup>R. J. Nemanich, J. T. Glass, G. Lucovsky, and R. E. Shroder, *J. Vac. Sci. Technol. A* **6**, 1783 (1988).
- <sup>31</sup>H. Hirai *et al.*, *Appl. Phys. Lett.* **71**, 3016 (1997).
- <sup>32</sup>N. Wada and S. A. Solin, *Physica B* **105B**, 353 (1981).
- <sup>33</sup>H. Windischmann, G. F. Epps, Y. Cong, and R. W. Collins, *J. Appl. Phys.* **69**, 2231 (1991).
- <sup>34</sup>B. D. Cullity, *Elements of X-Ray Diffraction* (Addison-Wesley, Reading, MA, 1959), p. 99.
- <sup>35</sup>T. Sharda, D. S. Misra, D. K. Avasthi, and G. K. Mehta, *Solid State Commun.* **98**, 879 (1996).
- <sup>36</sup>T. Sharda, D. S. Misra, and D. K. Avasthi, *Vacuum* **47**, 1269 (1996).
- <sup>37</sup>C. A. Davis, *Thin Solid Films* **226**, 30 (1993).
- <sup>38</sup>H. Windischmann, *J. Appl. Phys.* **62**, 1800 (1987).